Composites: Part A 140 (2021) 106193

Contents lists available at ScienceDirect

Composites Part A

journal homepage: www.elsevier.com/locate/compositesa

Hygrothermal ageing of pultruded GFRP profiles: Comparative study of unsaturated polyester and vinyl ester resin matrices

J.M. Sousa [a], M. Garrido [a,*], J.R. Correia [a], S. Cabral-Fonseca [b]

[a] CERIS, Instituto Superior Técnico, Universidade de Lisboa, Av. Rovisco Pais 1, 1049-001 Lisbon, Portugal
[b] Materials Department, Organic Materials Division (NMO), National Laboratory of Civil Engineering (LNEC), Av. do Brasil 101, 1700-066 Lisboa, Portugal

ARTICLE INFO

Keywords:
A. Polymer-matrix composites (PMCs)
B. Environmental degradation
D. Mechanical testing
E. Pultrusion

ABSTRACT

The durability of pultruded GFRP composites is critical to their performance in civil engineering applications, for which comprehensive and validated data is limited. To address this issue, this study presents an extensive experimental programme on the effects of hygrothermal ageing on the performance of pultruded GFRP profiles made of two alternative resin systems – unsaturated polyester (UP) and vinyl ester (VE) – both comprising identical fibre architecture. The ageing environments included immersion in demineralised and salt water at three different temperatures (20 °C, 40 °C, and 60 °C), and continuous condensation at 40 °C, for durations up to two years. Physical, viscoelastic and mechanical (tensile, flexural, in-plane and interlaminar shear) properties were assessed after a desorption period. As expected, the VE profile had overall better performance than the UP profile. After 24 months, the highest reductions in tensile strength occurred for water immersion at 60 °C, namely 45% and 33% for the UP and VE profiles, respectively. This paper provides a wealth of test data that can be used for degradation models for the prediction of their long-term mechanical property retention.

1. Introduction

The durability and long-term behaviour of fibre reinforced polymer (FRP) composites are a critical aspect of their performance for civil engineering applications, since (i) the required service life in civil infrastructure is generally over 50 years, and (ii) many knowledge "gaps" still need to be fulfilled regarding this specific industry [1]. Results obtained in previous studies conducted in FRP composites used in other industries (e.g., aerospace or naval), where more documentation and a better understanding were already obtained [1], show that several competing mechanisms may affect the durability of FRPs exposed to hygrothermal ageing conditions, such as: (i) additional cross-linking due to residual curing of the polymeric resin; (ii) secondary cross-linking between polymer chains and water molecules; (iii) swelling; (iv) micro-cracking; (v) plasticization; (vi) hydrolysis; (vii) leaching out of low molecular weight segments, and (viii) relaxation phenomena [2–6].

In the specific case of pultruded glass-FRP (GFRP) profiles, comprehensive and validated data on their durability is still relatively limited and a full understanding of the ageing and degradation mechanisms experienced by pultruded GFRP composites when subjected to different service conditions likely to be found in civil engineering applications has not yet been achieved. Most of the previous studies have focused mainly on tensile or flexural properties (e.g., [2,4,5,7]), leaving important knowledge gaps in what concerns in-plane shear or compression properties, both of which are equally important properties in the context of civil engineering applications of pultruded profiles. Furthermore, the thickness of laminates typically found in the literature is relatively low, often lower than 4 mm (e.g., [2,4,8]), being clearly lower than typical thicknesses found in structural-grade pultruded profiles. Moreover, the characteristics of the GFRP components can vary significantly, even for the same manufacturing technique (such as pultrusion), since the final products can result from a multitude of combinations of types of resin matrix and fibre reinforcement, fibre content and architecture (e.g., number and position of mats, unidirectional rovings and/or surface veils). Despite this, only a few studies have compared alternative resin systems with similar fibre reinforcement aged under the same conditions (e.g., [5,8,9]).

It is also important to highlight that experiments under accelerated ageing conditions are rarely longer than one year; among the few exceptions are the studies of Cabral-Fonseca *et al.* [5] and Lopez-Anido *et al.* [10]. Furthermore, systematic information regarding the "dry state" behaviour of pultruded GFRP profiles (*i.e.*, after a desorption

* Corresponding author.
E-mail address: mario.garrido@tecnico.ulisboa.pt (M. Garrido).

https://doi.org/10.1016/j.compositesa.2020.106193
Received 23 June 2020; Received in revised form 23 October 2020; Accepted 31 October 2020
Available online 6 November 2020
1359-835X/

period up to constant mass, following hygrothermal ageing) is very scarce [2], which is paradoxical, since most civil engineering applications (apart from submersed structures) are not typically in permanent contact with aqueous solutions during their service life, and are often subjected to relatively dry periods, during the warmer seasons, especially in mild climates.

Obtaining more comprehensive durability data, specifically derived from the type of laminates and conditions likely to be found in civil engineering applications is very important for design purposes, namely to allow the development of degradation models able to predict long-term retention of mechanical properties. The direct knowledge transfer from the aerospace and marine sectors is not straightforward, since the service life, the frequency and procedures of inspection and maintenance operations, and also the types of FRP materials used in most civil engineering structures usually present significant differences compared to those sectors.

To fulfil the above-mentioned gaps in the literature, the present study presents an extensive experimental programme to investigate the effects of hygrothermal ageing on the durability and long-term performance of two commercial pultruded GFRP profiles made of two alternative resin systems – unsaturated polyester and vinyl ester – both comprising the same fibre content and architecture. Specimens of the two types of profiles were subjected to different ageing environments, namely immersion in demineralised and salt water at three different temperatures (20 °C, 40 °C, and 60 °C), and continuous condensation at 40 °C for up to two years, and were then tested regarding their physical, viscoelastic and mechanical responses. Tests were performed after a desorption period, thus allowing to compare the permanent effects of hygrothermal ageing experienced by both profiles, due to the reversibility nature of some of the physical degradation mechanisms [11].

2. Experimental programme

2.1. Materials

Two types of "off-the-shelf" pultruded GFRP profiles (3 m long) were manufactured by company *ALTO Perfis Pultrudidos*. The profiles had rectangular cross-section of 33 × 5 mm^2, and were produced at an average speed of 0.25 m/min in a heated die where temperatures ranged between 130 °C and 165 °C. The laminates comprised E-glass unidirectional rovings with silane sizing and linear density of 4800 tex (typically corresponding to a filament diameter of ≈24 μm) in the core region, and two outer continuous strand mats (CSM) with weight of 450 g/m^2, embedded in either isophthalic unsaturated polyester (UP profile) or vinyl ester (VE profile) resins.

The UP resin was included in this study for being used in most civil engineering applications where environmental harshness in not a major concern. On the other hand, the VE resin was also included in this study as it is often preferred for applications in relatively harsh or corrosive environments. Both profiles had the same glass fibre content and architecture, thus allowing for a direct comparison of the durability performance of their resins.

2.2. Ageing environments

Different ageing environments were chosen to evaluate the susceptibility to degradation of pultruded GFRP profiles when exposed to typical conditions of civil engineering applications. Typical environments may include indoor conditions, but more frequently they involve wet environments, coastal areas and outdoor conditions, with exposure to varying temperature, moisture and UV radiation. Taking these factors into consideration, specimens of both types of profiles were subjected to the following environments, as detailed in Table 1: (i) immersion in demineralized water at 20 ± 3 °C, 40 ± 2 °C and 60 ± 2 °C; (ii) immersion in salt water at the same temperatures, and (iii) continuous condensation at 40 ± 2 °C and 100% relative humidity (RH).

Table 1
Ageing environments, durations, and conditions.

Ageing environments	Label	Duration [months]	Conditions[(a)]
Immersion in demineralised water	W20	0, 3, 6, 9, 12, 18, 24	T: 20 ± 3 °C
	W40		T: 40 ± 2 °C
	W60		T: 60 ± 2 °C
Immersion in salt water	S20	0, 3, 6, 9, 12, 18, 24	T: 20 ± 3 °C; 35 g/l NaCl
	S40		T: 40 ± 2 °C; 35 g/l NaCl
	S60		T: 60 ± 2 °C; 35 g/l NaCl
Continuous condensation	C40	0, 3, 6, 9, 12	T: 40 ± 2 °C; RH: 100%

[(a)]T: temperature; RH: relative humidity.

Investigations about the performance of the same GFRP profiles when exposed to outdoor ageing is presented elsewhere [12].

Immersion ageing in the above-mentioned media was based on ISO 175 standard [13], while the salt water concentration was selected as indicated in ASTM D 1141 standard [14]. The 20 °C nominal temperature was set as normal room temperature, corresponding to typical average temperatures encountered in mild Mediterranean climates.

Higher nominal temperatures of 40 °C and 60 °C were selected to accelerate the diffusion process and to promote the hygrothermal degradation mechanisms. These values were carefully set taking into account the need to remain well below the GFRP glass transition temperature (T_g), which was in the range of 106–112 °C for both UP and VE profiles [taken from onset of the storage modulus (E') curve obtained from dynamic mechanical analysis (DMA) results, *cf.* §3.1], in order to avoid or minimize any additional degradation mechanisms that may occur when such temperature is approached or exceeded [6,7].

The continuous condensation environment was achieved with a condensation chamber that combines the effects of moisture and temperature. Specimens were suspended inside the chamber, without contacting the chamber walls. Temperature and RH values were defined according to ISO 6270-1 standard [15].

Prior to ageing, only transverse cuts were made to the GFRP profiles, using a water-cooled diamond-tipped circular saw, to produce several profile segments. This was made in order to more accurately represent the bulk material and to minimize the length of exposed cut sections during ageing, which are preferable points for water ingress. After executing the longitudinal cuts, the profile segments (33 × 340 mm^2) were preconditioned until constant weight in a ventilated chamber at 80 ± 1 °C, according to ASTM D 5229 standard [16], before being exposed to the different ageing environments.

At predefined exposure times, the segments were removed from the ageing environments, and then cut with the same diamond-tipped circular saw to obtain specimens with geometries set by the standards corresponding to the different tests. In addition, the specimens were subsequently subjected to a desorption period, through conditioning until constant weight, using the same method described above, guaranteeing the aforementioned "dry-state". Finally, the specimens were placed in hermetically closed polyethylene recipients for transportation purposes and tested without further conditioning at controlled room temperature (20 ± 2 °C).

2.3. Characterisation methods

Both UP and VE profiles were subjected to several characterisation tests in order to determine their physical, viscoelastic and mechanical response when subjected to hygrothermal ageing, namely: (i) media diffusion, through gravimetric changes; (ii) thermo-mechanical behaviour, through DMA; and (iii) mechanical behaviour, by means of tensile, flexural, in-plane shear, and interlaminar shear tests. Characterisation

tests were conducted on each batch of test specimens after the predetermined periods specified in Table 1.

2.3.1. Gravimetric analysis

The mass variations during the hygrothermal ageing were assessed by means of gravimetric measurements. Specimens with dimensions 5 × 15 × 60 mm^3 were periodically removed from the recipients and, after wiping the superficial water from all surfaces, were immediately weighted using an analytical balance to determine the percentage of absorbed water, according to ASTM D 5229 standard [16]. Subsequently, the specimens were immediately returned to the recipient. Two specimens per ageing condition were considered, as preliminary tests provided very consistent measurements (insignificant error margin). These measurements were carried out with the purpose of comparing the sorption of the two types of profiles, and not with the goal of estimating the moisture content (as a function of time) of the specimens used in the remaining tests.

2.3.2. DMA

The temperature-dependent behaviour and T_g of the GFRP materials was assessed through DMA, according to parts 1 and 5 of ISO 6721 standard [17], using a DMA analyser from *TA Instruments*, model *Q800*. GFRP specimens with dimensions 5 × 15 × 60 mm^3 were tested in a three-point bending configuration at a constant frequency of 1 Hz and strain amplitude of 15 μm, from room temperature to 200 °C (in air), at a rate of 2 °C/min. The T_g was determined from the peak of the loss factor (tan δ) curve and from the storage modulus (E') curve as the extrapolated onset of its sigmoidal change, as per the definition of ASTM E 1640 standard [18]. Three specimens per ageing condition and duration period were tested.

2.3.3. Mechanical characterisation

As mentioned, the mechanical properties were determined through (i) tensile, (ii) flexural, (iii) in–plane shear and (iv) interlaminar shear tests. At least five specimens were tested for each material and type of test after ageing, and ten were tested for the initial characterisation of the unaged material.

The tensile properties of the GFRP laminates were determined according to parts 1 and 4 of ISO 527 standard [19] in specimens with 5 × 25 × 300 mm^3, without end tabs as these were deemed unnecessary taking into account that the failure modes observed were consistently located in the gauge section of the specimens; a clip-on extensometer was used to measure the tensile strains. The flexural properties of the GFRP laminates were assessed according to ISO 14125 standard [20] in test specimens with 5 × 15 × 150 mm^3; specimens were tested in a three-point bending configuration with a 100 mm span and the strain was obtained from the midspan deflection, which was measured using a displacement transducer. The in-plane shear properties were determined from V-notched beam tests according to ASTM D 5379/D 5379M standard [21], using a video-extensometer to measure the shear strains; the geometry of the specimens was 5 × 20 × 50 mm^3, comprising a 4 mm deep notch on both sides. The interlaminar shear strength of the GFRP laminates was determined in accordance to ASTM D 2344 standard [22] in specimens with 5 × 15 × 30 mm^3, tested in a 20 mm span.

2.3.4. Additional characterisation procedures

Additional chemical and physical tests were performed to fully characterise the unaged materials, namely: (i) chemical composition, through Fourier Transform Infrared (FTIR) spectroscopy; (ii) constituent materials proportion, through calcination; and (iii) density, through the immersion method.

Infrared spectra of both GFRP materials were assessed for initial characterisation by means of FTIR spectroscopy in the 450–4000 cm^{-1} region. For these measurements, powder samples, scraped from the surface of test specimens, were mixed with dry spectroscopic grade potassium bromide and pressed into pellets. The results of 32 scans were collected and averaged at a spectral resolution of 4 cm^{-1}, according to ASTM E 1252 standard [23]. This technique was used to provide initial detailed data on the surface constituents of the GFRP material.

The glass fibre content was determined by the calcination method, described in ISO 1172 standard [24], in three specimens with 20 × 10 × 5 mm^3. The density of the materials was determined in accordance with method A of ISO 1183 (Part 1) standard [25], in three 0.5 mm^3 cubic specimens with 0.1 mg.

3. Results and discussion

3.1. Characterisation of reference (unaged) GFRP materials

The experimental results of physical-chemical characterisation of both profiles before ageing are listed in Table 2 (average ± standard deviation values are listed, where applicable).

The chemical composition of both materials, determined by FTIR spectroscopy and illustrated in Fig. 1, was fairly similar. The intensity and location of the peaks confirmed the presence of the ester group, as well as aromatic and aliphatic molecular structures, common in both unsaturated polyester and vinyl ester polymers. The FTIR spectra also show the presence of calcium carbonate (filler) and silica (from E-glass fibres). However, comparing both spectra it is possible to observe that the C═O peak located at 1730 cm^{-1} is more intense in the UP profile, which is indicative of the higher amount of ester groups present in unsaturated polyester in their chemical composition.

The glass fibre content and density of the UP profile were slightly lower when compared with the VE profile. The values obtained for these two physical properties are in the typical range for this type of structural grade profiles [5].

Fig. 2 presents representative DMA curves [storage modulus (E'): left axis, dashed lines; and loss factor (tan δ): right axis, continuous lines]. The E' curves presented the typical sigmoidal shape usually found in polymers and FRP composites, with the onset of the reduction of E' occurring at 112 °C and 107 °C for the UP and VE profiles, respectively.

The tan δ curve exhibited peaks at a higher temperature range of 124–137 °C, with the curve peaks for the VE and UP profiles corresponding respectively to the lower and upper bounds of that interval. In

Table 2
Physical and chemical properties of the unaged GFRP profiles.

Property	Method		UP profile	VE profile
Chemical composition	FTIR	FTIR spectra consistent with unsaturated polyester or vinyl ester, with presence of calcium carbonate and silica		
Glass fibre content	Calcination	[% of mass]	65.3 ± 1.8	67.9 ± 1.8
Density	Immersion	[g/cm^3]	1.92	1.96
T_g	DMA	T_g (E'$_{onset}$) [°C]	112.3 ± 3.6	106.6 ± 1.3
		T_g (tan δ) [°C]	136.6 ± 0.4	124.1 ± 0.3
Mechanical properties	Tensile response	σ_{tu} [MPa]	479.5 ± 28.9	430.0 ± 33.8
		E_t [GPa]	37.4 ± 2.3	39.2 ± 0.5
		ε_{tu} [–]	0.014 ± 0.001	0.012 ± 0.001
	Flexural response	σ_{fu} [MPa]	552.6 ± 40.2	561.1 ± 16.8
		E_f [GPa]	21.4 ± 2.3	23.0 ± 0.8
		ε_{fu} [–]	0.024 ± 0.003	0.021 ± 0.001
	In-plane shear	τ_{max} [MPa]	53.7 ± 1.9	67.6 ± 2.1
		G [GPa]	3.0 ± 0.5	3.8 ± 0.6
		γ_u [–]	0.035 ± 0.006	0.035 ± 0.005
	Interlaminar shear	σ_{sbs} [MPa]	34.7 ± 4.5	37.8 ± 1.7

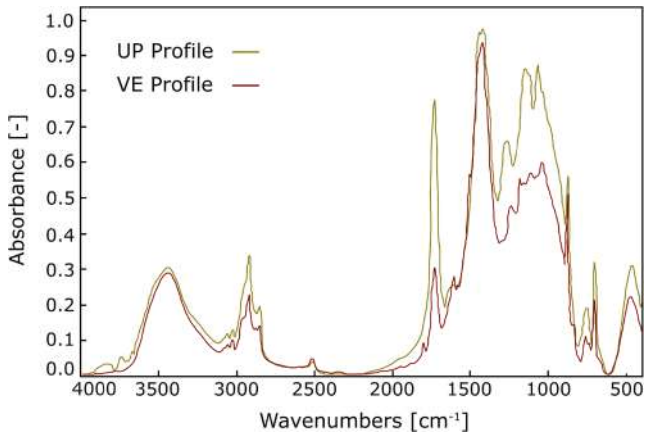

Fig. 1. FTIR spectra of unaged UP and VE profiles. (For interpretation of the references to colour in this figure legend, the reader is referred to the web version of this article.)

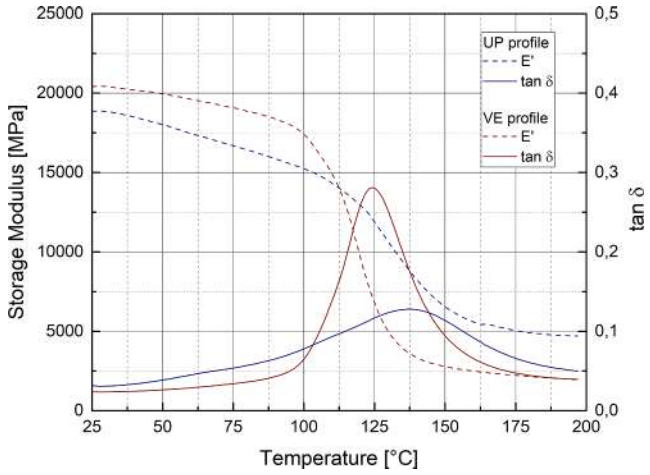

Fig. 2. DMA experimental curves for unaged UP and VE profiles. (For interpretation of the references to colour in this figure legend, the reader is referred to the web version of this article.)

fact, the T_g estimates obtained from both the tan δ curve and the onset of the E' curve were slightly higher for the UP profile. Additionally, the peak value of tan δ was significantly lower for the UP profile than for the VE counterpart, in agreement with the denser molecular arrangement of the ester groups in the polymeric chain of the UP profile, which makes it less sensitive to molecular rearrangement when exposed to higher temperatures [5].

Fig. 3 presents representative stress *vs.* strain curves (or stress *vs.* displacement curves for interlaminar shear) obtained from the different mechanical tests. As expected, for both profiles, the mechanical tests indicated a general linear elastic behaviour up to failure; the single exception was the in-plane shear tests, where the material presented a progressive stiffness reduction (non-linear behaviour) after an initial linear response. The average mechanical properties obtained for both profiles are listed in Table 2. Overall, the VE profile presented higher elastic properties (stiffness), which is visible in Fig. 3. Regarding flexural, in-plane shear, and interlaminar shear strength, the two profiles presented similar values, slightly higher in the VE profile. However, the UP profile exhibited superior performance regarding tensile strength when compared to the VE profile; these relative differences (~10%) were attributed to a worse fibre-matrix interaction with the vinyl ester resin used in the pultrusion of the VE profiles.

Fig. 4 illustrates the typical failure modes observed in the mechanical tests, which were as expected and quite similar for both types of profiles. Tensile failure [Fig. 4(a)] started with rupture of the CSM outer layers, followed by progressive rupture of the unidirectional glass fibres and delamination. Flexural failure started in the lower outer layer [*cf.* Fig. 4 (b)], where tensile stresses are maximum, and progressed to the upper part of the section causing rupture in the longitudinal fibres. In-plane shear failure [Fig. 4(c)] was characterised by the formation of a vertical crack between the notched edges, damaging both the matrix and the fibres (in the transverse direction). Finally, the interlaminar shear test caused failure to occur in the matrix at the central part of the specimen, and the consequent interlaminar delamination [*cf.* Fig. 4(d)]. It is also worth mentioning that the failure modes were unaffected by hygrothermal ageing, while the mechanical properties suffered considerable variations, as detailed ahead.

3.2. Sorption behaviour

Fig. 5 shows for both profiles their mass variation as a function of the square root of exposure time, for the different hygrothermal environments – immersions in demineralized and salt water at different temperatures (20, 40 and 60 °C) and continuous condensation at 40 °C.

Overall, mass uptake in the different ageing conditions showed a roughly approximated Fickian response. In fact, for both profiles water diffusion was significantly higher in earlier periods and approximated nearly constant values at the later periods. However, it is well known that water uptake can deviate from purely Fickian behaviour during longer exposure periods, where effects such as polymer relaxation may occur, causing differences from the theoretical response. This appears to be the case for some of the exposure environments, especially at higher temperatures (e.g., W60 and S60). In such cases, the water content is seemingly absorbed by the resin due the redistribution of voids and free volumes in the polymer network that are created through swelling effects caused by penetrant molecules. In addition, these molecules can force macro-molecular movement, causing even more water absorption by the polymer [26,27].

In general, as expected, the UP profile had higher mass uptake in almost all ageing environments (excluding S20), when compared to the VE profile, due to the chemical nature of both matrix polymers, as pointed out by Chin *et al.* [28] and Cabral-Fonseca *et al.* [5]. According to those authors, moisture diffusion into the polymeric matrix occurs in different ways, namely in terms of (i) moisture profile throughout the thickness, (ii) water uptake capacity and (iii) moisture ingress rate; these depend upon several microstructural and molecular aspects (*i.e.*, molecular structure polarity and degree of cross-linking). The higher UP sorption is highlighted in Table 3, where the maximum weight gain content (M_{max}) measured for each environment and respective time (t) are listed.

As expected, a clear and consistent temperature effect was noted in the weight changes of both profiles, with higher immersion temperatures corresponding progressively to higher water uptake, which is consistent with results reported in several previous works (e.g. [2,4–6]). For instance, considering the VE profile [*cf.* Fig. 5(b)], water uptake at 111 $h^{1/2}$ was 0.46%, 0.61% and 0.75% respectively for W20, W40, and W60 environments. Unlike other studies (e.g. [5,6,29,30]), mass uptake was not reverted at some point (due to mass loss by extraction of low molecular weight segments), even at higher temperatures.

For both types of profiles, when comparing results for both demineralised water and salt water at the same temperatures, the mass uptake was higher in the former medium. According to Jones [31], this effect can be attributed to the cross-linked polymeric matrix behaviour, enabling water movements and haltering large inorganic ions, thus acting as a semipermeable medium. Previous studies [5,32] also reported that the presence of salts (such as NaCl) in immersion media results in a reduction of the saturation value.

Continuous condensation at 40 °C, when compared to water immersions at the same temperature, involved a levelling off, with a

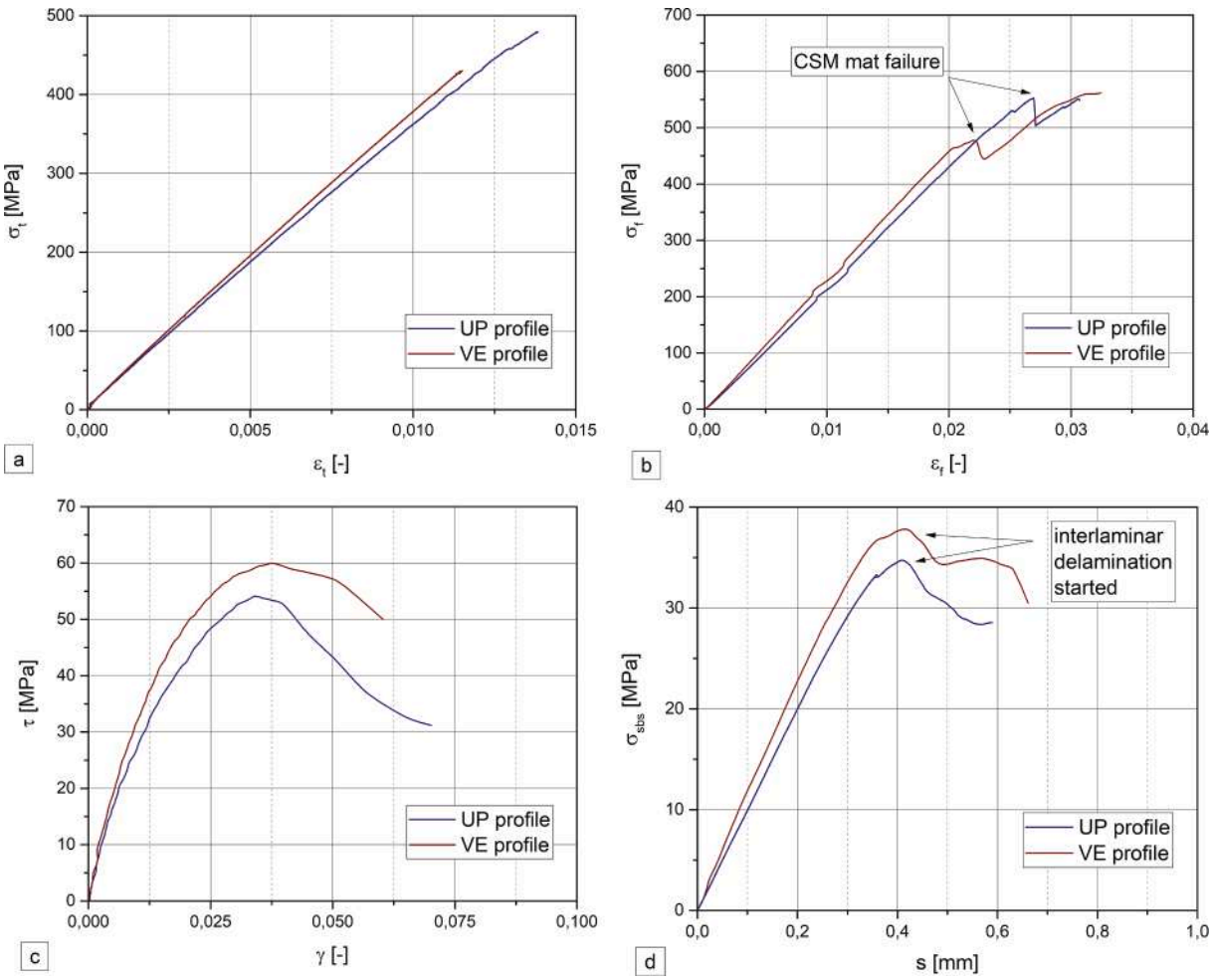

Fig. 3. Representative experimental curves for different mechanical properties: (a) tensile; (b) flexural; (c) in-plane shear; and (d) interlaminar shear. (For interpretation of the references to colour in this figure legend, the reader is referred to the web version of this article.)

saturation stage being reached clearly at lower exposure periods (around 50 and 25 $h^{1/2}$ for both UP and VE profiles, respectively) and for lower water uptake values (0.55% and 0.35%, respectively). However, in the earlier periods, during which higher diffusion rates were observed, the absorption for continuous condensation was comparable to that in demineralised water and salt-water immersion. These results are in accordance with previous findings [4,5].

3.3. Thermo-mechanical response

Fig. 6 shows representative DMA curves [storage modulus (E'): left axis, dashed lines; and loss factor (tan δ): right axis, continuous lines] obtained for unaged and aged profiles subjected to the different ageing environments for the selected periods. Unfortunately, the results obtained from DMA tests for the last two batches of the UP specimens (*i.e.*, at 18 and 24 months of ageing) were anomalous and were discarded. Note that salt water and continuous condensation environments are not represented; in fact, for both UP and VE profiles the behaviour in those environments was fairly similar when compared to demineralised water immersion at the same temperature (the results represented here).

Concerning water immersion in both profiles, regardless of the immersion time and temperature, the E′ curves present the sigmoidal shape typical of FRP materials: after a glassy plateau, the storage modulus drops (more steeply for the VE profile than for the UP profile) up to approximately 10–20% of the initial values. The curve shape reflects mainly the changes in the viscoelastic polymer matrix (progressing from a glassy to an elastomeric state), since the glass fibres do not suffer stiffness reduction in this temperature range [5] and did not seem to be affected by ageing; some deviations occurred (e.g., Fig. 6 (a), E' curve at 6 months), which consisted of two inflexion changes before the curve drop, first decreasing and subsequently increasing the storage modulus values. It is important to add that this deviation only occurred in a few specimens and periods of time. Nonetheless, this fact can be attributed to residual water molecules that were still trapped inside the specimens (even considering the drying process) gradually contributing to plasticization and subsequently evaporating, since it occurred for temperatures approaching 100 °C.

Considering 25 °C as a representative temperature of the glassy plateau, an initial decrease of storage modulus can be identified in both profiles due to hygrothermal ageing. This decrease was smaller for the UP profile following W20 exposure, where a progressive lowering can be seen up to 12 months of ageing, followed by a later stabilisation in the subsequent periods. This effect was more pronounced at higher temperatures and can be attributed, as mentioned, to the remaining absorbed water acting as a plasticizer [11]. Regarding the VE profile, this decrease was steeper right after 2 months of ageing regardless of the exposure temperature. Grammatikos *et al.* [6] observed this tendency in pultruded UP profiles at 20 °C; however, at 40 °C, an initial drop was reported followed by an increase that exceeded the unaged values; at 60 °C, this increase occurred right after 28 days of ageing and this trend continued for the remaining period of the study. These differences in results can be attributed to the different "dry" *vs.* "wet" conditioning. However, Cabral-Fonseca *et al.* [5] reported general similar trends for the E' curve of comparable profiles tested in a wet condition.

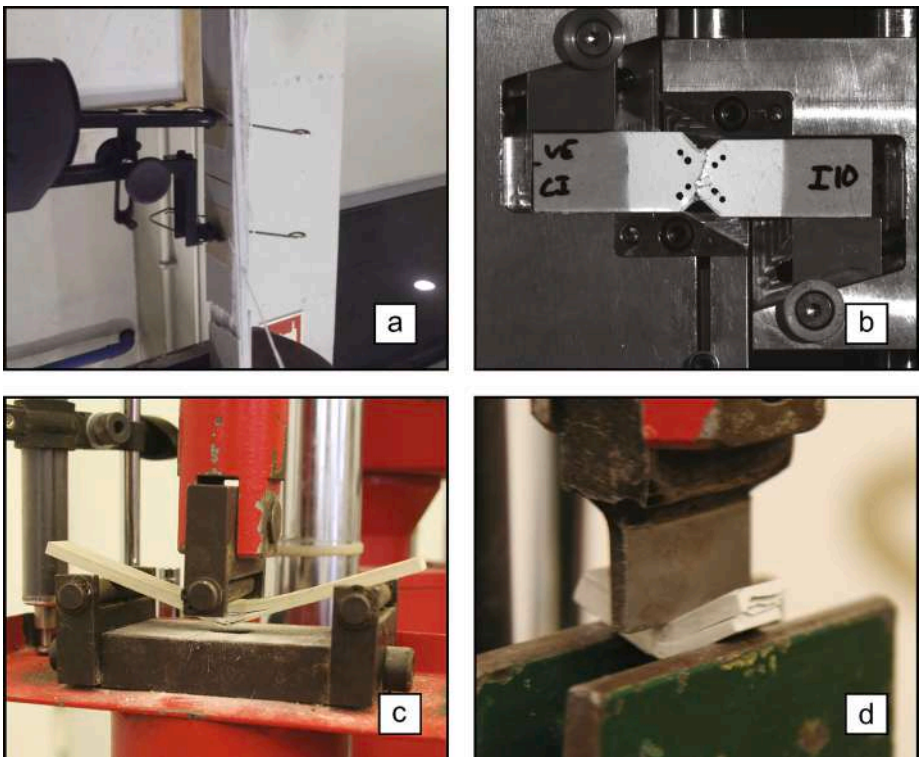

Fig. 4. Typical failure modes in the different mechanical tests: (a) tensile; (b) in-plane shear; (c) flexural; and (d) interlaminar shear. (For interpretation of the references to colour in this figure legend, the reader is referred to the web version of this article.)

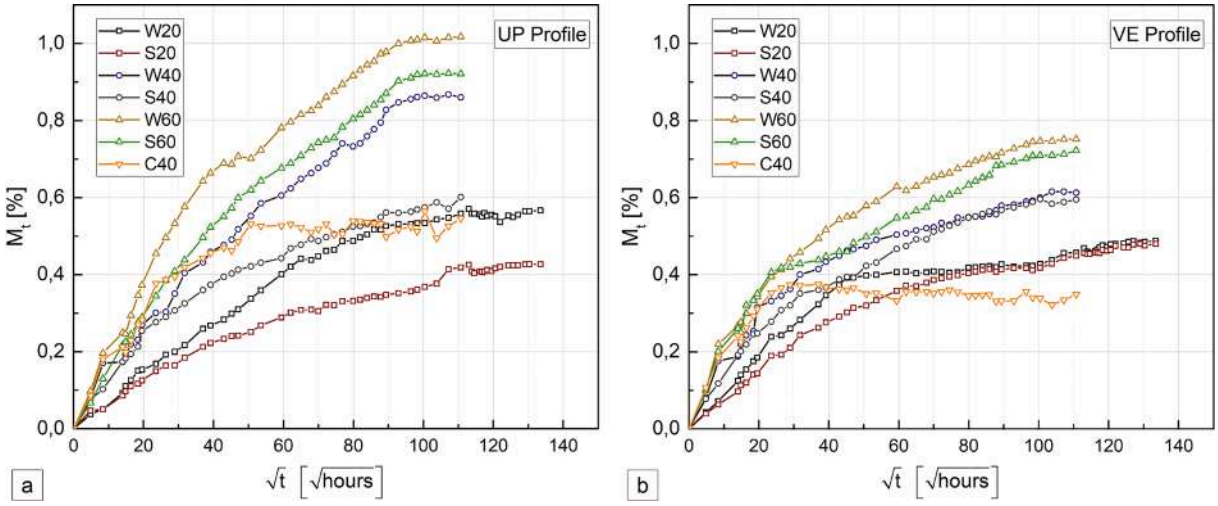

Fig. 5. Mass uptake during hygrothermal ageing for (a) UP and (b) VE profiles (representative curves). (For interpretation of the references to colour in this figure legend, the reader is referred to the web version of this article.)

Table 3
Maximum experimental weight changes and time elapsed until their occurrence.

Profile		W20	S20	W40	S40	W60	S60	C40
UP	M_{max} [%]	0.57	0.43	0.87	0.60	1.02	0.92	0.56
	t [days]	532	743	479	511	511	479	420
VE	M_{max} [%]	0.49	0.48	0.62	0.60	0.75	0.72	0.37
	t [days]	743	743	449	420	511	511	57

In addition, concerning the UP profile, the tan δ curve presented a right shift that occurred progressively up to 12 months. This shift was significantly temperature-dependent and was associated with an increase of the T_g estimate. Similar effects have been reported in previous works, but only for higher temperatures [5] or lower exposure times [11], and have been attributed to post-curing phenomena. However, the main difference between the studies lies in the drying procedure, which, in the present study, should have contributed to accentuate the post-curing effects, while attenuating some of the physical degradation (plasticization) that the specimens might have suffered, both effects contributing positively to this change. Post-cure is bound to occur during hygrothermal ageing of GFRP profiles, especially at higher temperatures, a process that is well documented [5,7,11,33]. The tan δ curves also presented some widening of the base, which seemed to increase with temperature, and suggested that some changes occurred at

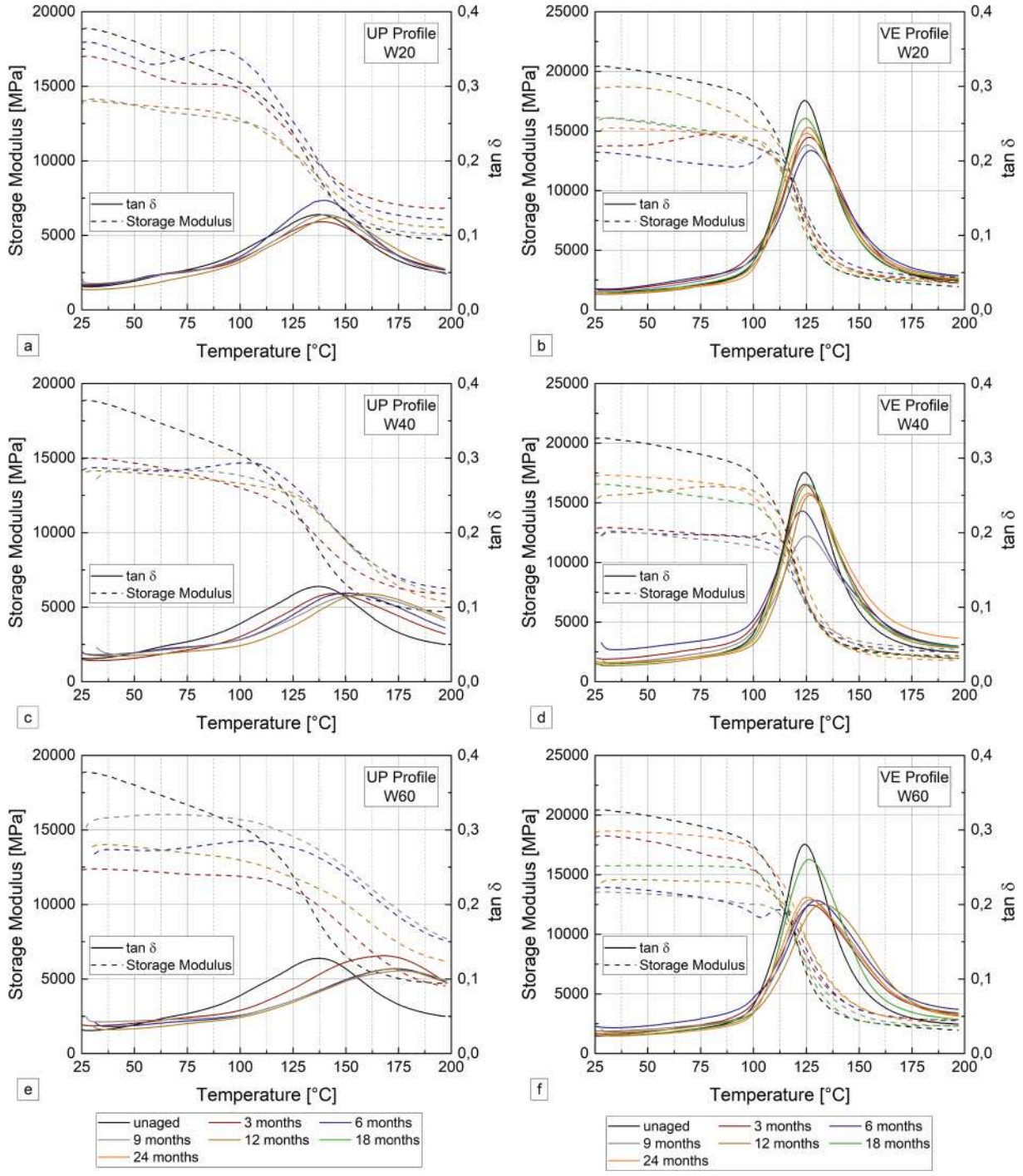

Fig. 6. DMA curves for demineralised water immersion at different temperatures and periods of time: at 20 °C for (a) UP and (b) VE profiles; at 40 °C for UP (c) and VE (d) profiles; at 60 °C for UP (e) and VE (f) profiles (representative curves). (For interpretation of the references to colour in this figure legend, the reader is referred to the web version of this article.)

the molecular structure level.

Concerning the VE profile, few changes occurred in the tan δ curve, except some progressive lowering of the curve height, which was also more noticeable at higher temperatures; this suggests the occurrence of post-cure phenomena, also reported by Karbhari [11]. The results for salt water immersion and continuous condensation were very similar to those discussed above, regarding the main trends of variation and the corresponding T_g values. These are presented in Fig. 7, which plots the changes in T_g estimates (average ± standard deviation) obtained from (i) the peak of the tan δ curve ($T_{g,\tan\delta}$), and (ii) the onset of the drop in the E' curve ($T_{g,E'onset}$).

For the UP profile, water immersion showed a general increasing trend of T_g from the unaged values up to 12 months, which was accentuated with temperature. This effect was clearer in $T_{g,\tan\delta}$, which showed increases of 5%, 17% and 27% for W20, W40 and W60 environments, respectively.

Since the matrix could have been not fully cured (although produced by pultrusion and subjected to post-curing), the degradation suffered by the ageing mechanisms may have resulted in a competing process with the post-curing phenomenon. In fact, the higher temperature may have

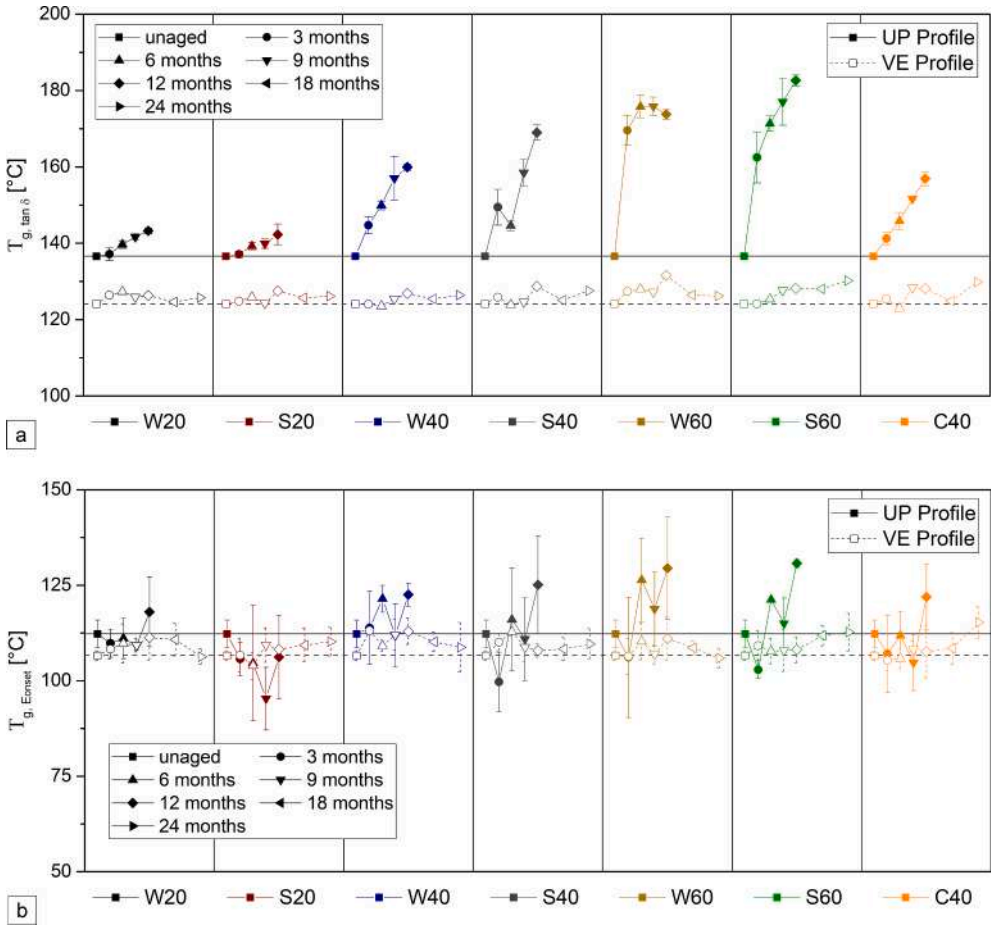

Fig. 7. Variations of the glass transition temperature for the different ageing environments and profiles: (a) $T_{g,\tan\delta}$, and (b) $T_{g,E'onset}$. (For interpretation of the references to colour in this figure legend, the reader is referred to the web version of this article.)

also contributed to these post-curing effects, attenuating and even compensating for the overall degradation.

Salt water and continuous condensation showed the exact same trends when compared to immersion at the same temperature (slightly higher increase of T_g for S40 and S60, compared to W40 and S60, respectively). Moreover, the same overall trend of increasing T_g (with some fluctuations for the salt water immersions) can also be found in the $T_{g,E'onset}$ for the UP profile, although with slightly lower increases (5%, 9% and 16% for W20, W40 and W60 at 12 months, respectively) and coupled with some irregular drops. This non-monotonic pattern of variation of the T_g, also reported by other authors [11], reflects the complexity of the above-mentioned competing effects of hygrothermal ageing.

Regarding the VE profile, little changes occurred in $T_{g,\tan\delta}$, with some insignificant increases at the higher temperatures (maximum of 4%) for the later exposure periods. The variation was less dependent from the immersion temperature, and less significant when compared to the UP profile, which is in accordance with previous investigations [5]. Consistency of the results obtained for water, salt water and continuous condensation is also observed, including for the different temperatures (in case of immersions). The $T_{g,E'onset}$ presented similar variation compared to the $T_{g,\tan\delta}$ (*i.e.*, small variations). Comparing with the results obtained for the UP profile, the nature of VE polymer (less ester groups, positioned in the extremities of the molecular structure, and a "tougher" chain) makes it less susceptible to water degradation by hydrolysis [34], and also more resistant to the above-mentioned plasticization mechanisms [5]. As such, the same positive effects due to drying resulted in a very stable T_g performance, even at higher temperatures (up to 60 °C).

In summary, in the present study, less overall degradation on T_g has been found for both profiles when comparing to other investigations [4–6,11,28]. As already discussed, this was most likely due to the drying process, which allowed to attenuate some degradation mechanisms and promote a competing post-curing effect. Altogether, this resulted in fluctuations in the T_g as a function of the exposure period, which was more evident in the UP profile.

3.4. Tensile response

Fig. 8 depicts the stress *vs.* strain curves for representative specimens of both profiles subjected to one of the ageing environments (W60 – the harsher), as an example, where the ageing effects on both properties are evident. Although the failure mode (*cf.* §3.1) was the same throughout the different ageing periods, hygrothermal ageing affected both tensile strength (σ_t) and modulus (E_t).

The effects of hygrothermal ageing on the tensile strength and modulus of the UP and VE profiles for all ageing environments (average ± standard deviation) are shown in Fig. 9.

Regarding the **UP profile**, the global negative effect of water uptake on the tensile properties is quite evident. General progressive reductions occurred for both properties and they were clearly temperature dependent. The results obtained indicate that irreversible degradation mechanisms, such as hydrolysis, took place. In addition, the tensile strength of the UP profile presented a higher initial reduction at 3 months, corresponding to the initial period where higher water uptake also occurred. Tensile strength reductions between 8–12%, 18–21%, and 21–28% occurred for immersions at 20 °C, 40 °C, and 60 °C, respectively. Afterwards, it increased (as mentioned) or stabilised for W20 and S20,

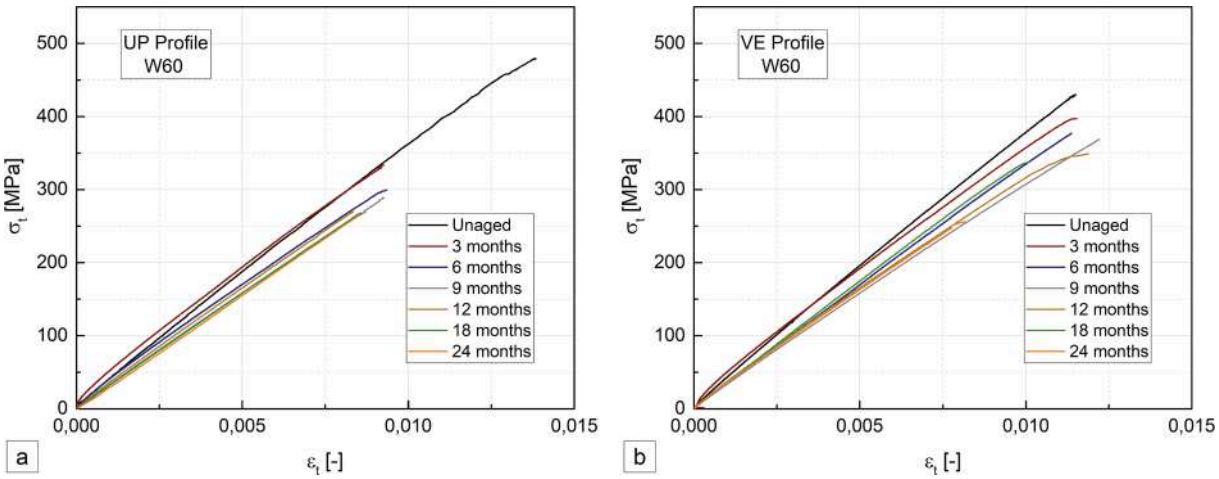

Fig. 8. Tensile stress *vs*. strain curves at different ageing times for immersion in water at 60 °C: (a) UP and (b) VE profiles (representative curves). (For interpretation of the references to colour in this figure legend, the reader is referred to the web version of this article.)

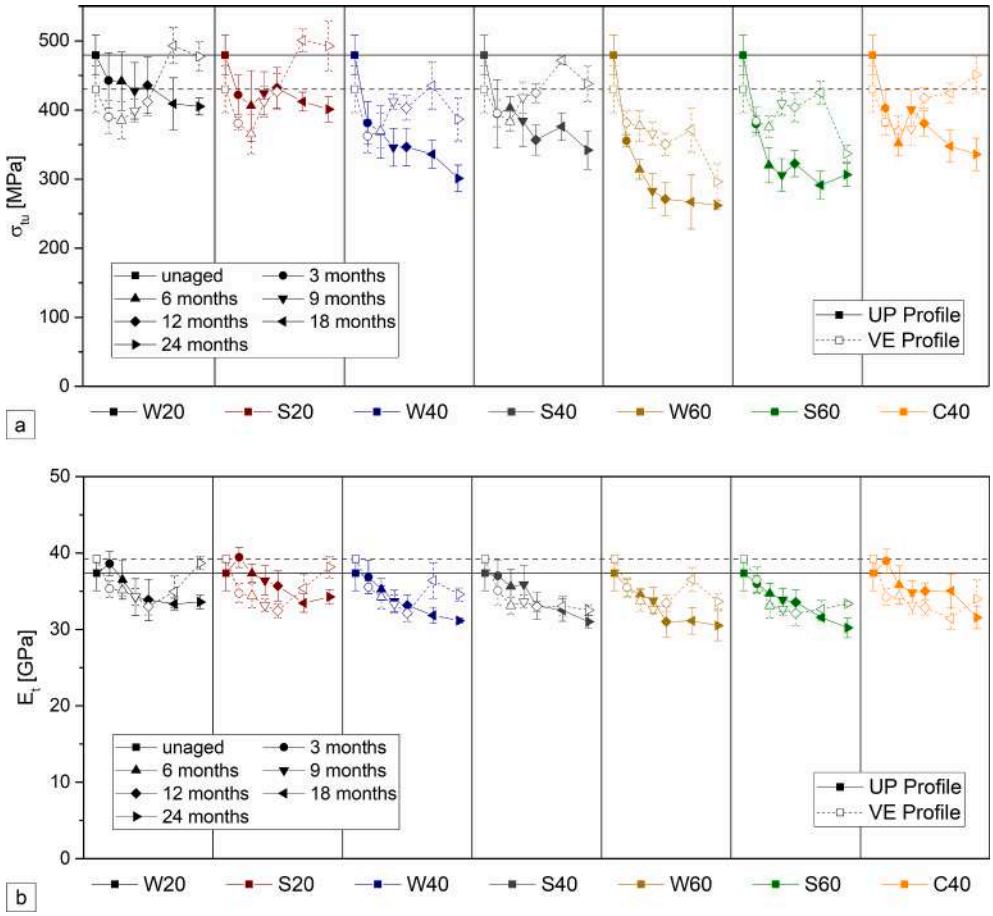

Fig. 9. Variations of tensile (a) strength and (b) modulus for both profiles in the different ageing environments. (For interpretation of the references to colour in this figure legend, the reader is referred to the web version of this article.)

respectively, which most likely stemmed from the desorption period that should have attenuated some reversible degradation, such as that due to plasticization, and possibly increased the post curing effects. However, the decreasing trend was still noted at the remaining ageing environments, although at a lower rate, suggesting that the high temperatures continued to promote irreversible degradation mechanisms, such as hydrolysis. These competing degradation mechanisms have already been reported in previous works [2,4,7,11,28,31].

In agreement with the water uptake behaviour, salt water environments caused similar changes when compared to water at the same temperature, although causing less overall degradation (especially at higher temperatures). In addition, the continuous condensation environment also presented similar trends when compared to immersions at the same temperature.

After 24 months of hygrothermal ageing, reductions in the tensile strength of the UP profile of 15–16%, 29–37%, 36–45% and 30% were

observed for immersions at 20 °C, 40 °C, 60 °C and continuous condensation at 40 °C, respectively.

The tensile modulus of the UP profile was less affected – despite not showing a higher initial drop (as observed for the tensile strength), it presented a general decaying trend over the time of exposure, with a steady reduction trend with almost no signs of recovery (apart from 3 months at W20, S20, and C40, for which the tensile modulus was 3–5% higher than that of unaged specimens). Although the reduction of tensile modulus was more pronounced for higher temperatures, this effect was not so evident when compared to tensile strength. Salt water immersions had roughly the same effects as demineralised water immersions and the same can be said for continuous condensation at 40 °C compared to immersion at the same temperature.

After 24 months of exposure, the tensile modulus of the UP profile decreased by 8–10%, 16–17%, 18–19%, and 16% for immersions at 20 °C, 40 °C, 60 °C and continuous condensation at 40 °C, respectively.

Different effects were found in the **VE profile**. In fact, apart from immersions at 60 °C (W60 and S60), in all ageing environments the tensile strength presented an early decrease up to 9 months, which was of the same order of magnitude for the 20 °C and 40 °C immersions (10–15%, 11–14% reductions, respectively), and was followed by a progressive increase up to 24 months of exposure, even exceeding the unaged values for some environments. This increase probably stemmed from the already mentioned competing mechanisms of residual curing, and seemed to be more significant in the lower temperature environments. In the last exposure period at W40, this increase was not observed, with tensile strength presenting a slight reduction. For C40 exposure, similar changes were found compared to W40 and S40. Immersions at 60 °C caused the highest degradation in tensile strength: for W60 there was an almost monotonic decrease during the whole exposure period and for S60 a general reduction trend took place (with a slight increase from 12 to 18 months), suggesting that irreversible degradation occurred, being more relevant at higher temperatures. After 24 months of hygrothermal ageing, the tensile strength increased by 11–15%, 2% and 5% for the 20 °C immersions, S40, and C40 respectively. On the other hand, reductions of 10%, 31% and 22% were observed for W40, W60 and S60 environments at the same period. Overall, compared to the UP profiles, the tensile strength of the VE profile was clearly less affected, which is consistent with the lower prevalence of hydrolysis phenomena in the VE resin, already referred in section 3.3, about the DMA results.

The tensile modulus of the VE profile presented an initial higher drop at 3 months of ageing for all environments, a subsequent lower reduction throughout the exposure time, and then tended to a plateau at later stages of exposure. Immersions at 20 °C and W40 also showed some property recovery after 12 months. In this case, the temperature dependency of the tensile modulus variation was not evident, *i.e.*, this property exhibited similar degradation levels for lower and higher temperatures of immersion (despite the last periods at 20 °C). Similarly to the tensile strength (and tensile properties of the UP profile), and as expected, salt water and continuous condensation had the same correlations with immersion in demineralised water at the same temperatures. After 24 months, the tensile modulus presented reductions of 1–3%, 12–17%, 14–15%, and 13% for immersions at 20 °C, 40 °C, 60 °C and continuous condensation at 40 °C, respectively.

The same degradation mechanisms that were referred to affect the tensile properties of the UP profile should have also affected the VE profile. The differences between the magnitudes and trends of the degradation experienced by their tensile properties are attributed to (i) the higher chemical resistance of the VE profile, together with (ii) the reduction of the physical degradation mechanisms due to the drying process, which made the post-curing phenomena more relevant in the VE profile.

These results are consistent with findings reported in previous works on the tensile properties of similar pultruded profiles [5,6,8]. However, the degradation levels in the present study were lower, and the performance increase exhibited by the VE profile was higher, and this should be attributed to the desorption period before testing the specimens. Chu *et al.* [2] also studied pultruded VE-GFRP and reported similar decaying trends, which were also more significant at early stages, in agreement with the results obtained here. However, in that study, despite the occurrence of post-curing, noted in DMA tests, its effects were not visible in the retention of tensile properties. It is also worth mentioning that the desorption period used in that study did not cause significant differences in tensile properties retention. These differences to the present study may be due to dissimilarities in specimen thickness (significantly thinner in [2], with only 1.6 mm).

3.5. Flexural response

Fig. 10 depicts stress *vs.* strain curves for representative specimens of both profiles exposed to one of the ageing environments (W60), as an example of the changes in flexural strength (σ_f) and stiffness (E_f). Despite displaying the same failure mechanisms for all ageing periods, hygrothermal ageing affected the flexural properties of the profiles.

A generalised reduction of flexural strength can be identified with the increase of exposure time, while stiffness presented irregular (non-monotonic) variations with some signs of recovery. It is also interesting to note that the constitutive behaviour in the brink of collapse changed during ageing: while for unaged specimens and for shorter ageing durations, there was some stress recovery after the tensile failure of the lower (tensioned) CSM, for the latter periods of exposure (where higher degradation is expected to occur) the flexural stress did not increase after the failure of the lower CSM. This is considered indicative of the degradation of the fibre-matrix adhesion, as well as of the interfaces between layers of fibre reinforcement.

The effects of all types of hygrothermal ageing environments on the flexural strength and modulus of the UP and VE profiles (average ± standard deviation) are shown in Fig. 11.

In general, as for the tensile strength, the level of degradation in flexural strength for both profiles increased with the temperature of the immersion media. Both profiles exhibited similar behaviour when comparing immersions at 20 °C, with an initial gradual and progressive reduction, followed by a stabilisation trend after 12 months of ageing. Similar trends were observed for the higher temperature environments, however with a steeper and more pronounced initial reduction. In the 40 °C and 60 °C ageing environments similar effects were found for both profiles, consisting of a higher initial reduction of flexural strength up to 9 months (27–31%) and then a slower reduction up to 24 months.

Exposure to continuous condensation again produced roughly similar effects to immersion environments at the same temperature, and the flexural strength after water immersions were usually slightly higher when compared to salt water immersions. In previous studies [5,8,9,29] that analysed the flexural properties of GFRP profiles made of UP and VE resins and in which a desorption period was not considered, higher overall reductions were found due to hygrothermal aging, especially in the VE profile. This fact is attributed to the drying effects already discussed (regarding the tensile properties) that have been confirmed to contribute to attenuate and eventually recover some of the physical degradation mechanisms, such as plasticization [11].

Unlike the tensile results, no apparent strength recovery was found in the VE profile, which should stem from the higher influence of the polymer matrix, and especially of the fibre-matrix interface condition, in the flexural properties when compared to the more fibre-dominated tensile properties. These trends are in accordance with previous results [5]. In any case, as expected, the VE profile exhibited less reduction in flexural strength than the UP profile, especially at 40 °C and 60 °C. After 24 months, the flexural strength of the UP profile presented reductions of 9–15%, 23–24%, 39–48%, and 30% for immersions at 20 °C, 40 °C, 60 °C, and continuous condensation at 40 °C, respectively; in the VE profile those figures were 9–10%, 18–20%, 23–37%, and 16%.

Regarding flexural modulus, similarly to the tensile modulus, a more

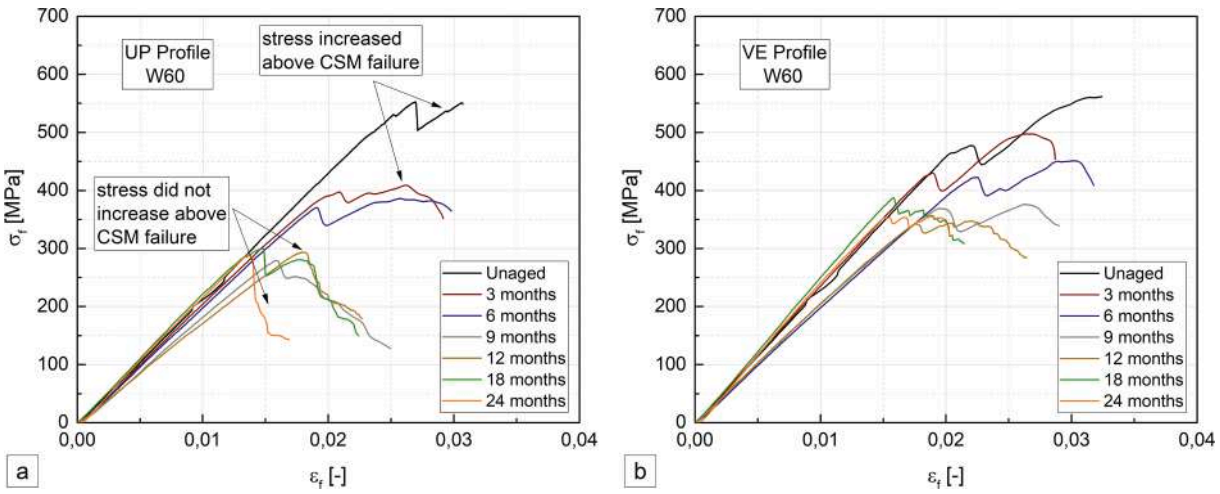

Fig. 10. Flexure stress-strain curves at different ageing times for immersion in water at 60 °C: (a) UP and (b) VE profiles (representative curves). (For interpretation of the references to colour in this figure legend, the reader is referred to the web version of this article.)

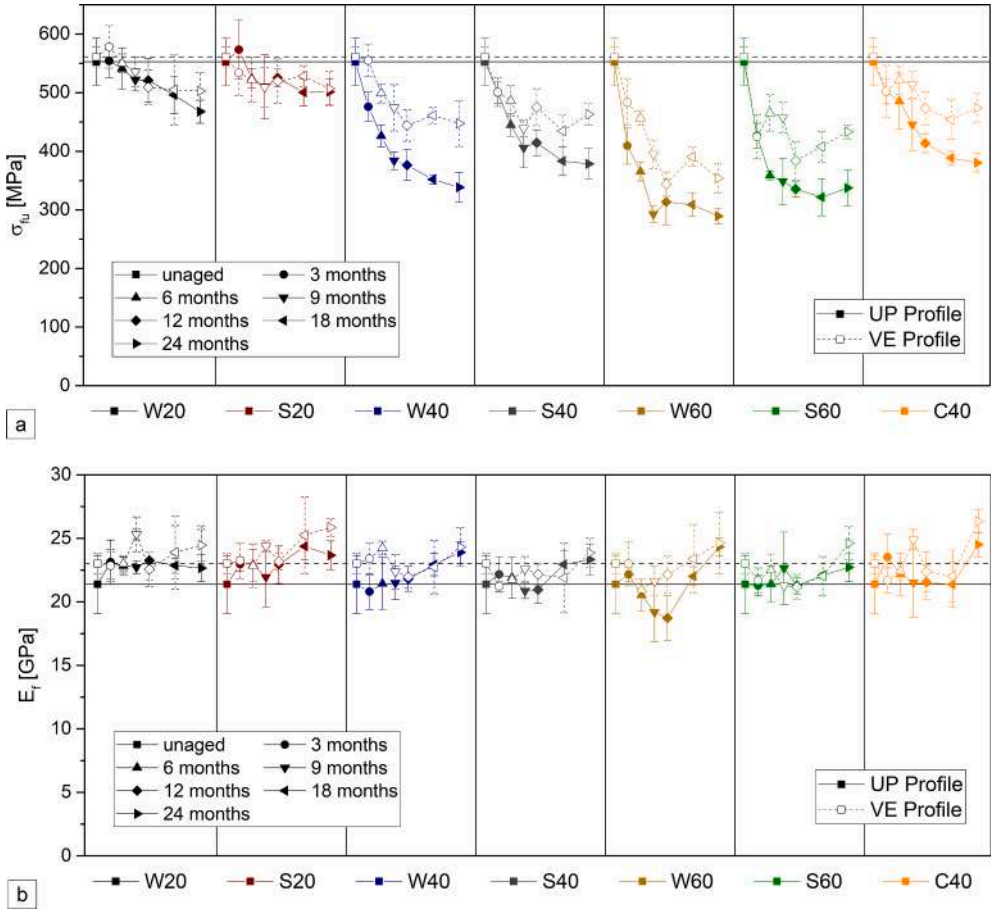

Fig. 11. Variations of (a) flexural strength, and (b) modulus for both profiles in the different ageing environments. (For interpretation of the references to colour in this figure legend, the reader is referred to the web version of this article.)

irregular variation (non-monotonic) was found for both profiles. Overall, the VE profile displayed better performance and usually presented higher stiffness than the UP profile. However, since the unaged flexural modulus was also higher, their moduli retentions were similar. Temperature did not seem to have a significant effect in the flexural modulus of both profiles. After 9 months, some property recovery can be identified, which should be associated with the aforementioned post-curing effects. This recovery is more evident in the UP profile, being consistent with the DMA test results. After 24 months of hygrothermal ageing, the flexural modulus of the UP profile presented 6–11%, 9–11%, 6–13% and 15% increase when compared to the unaged values, for immersions at 20 °C, 40 °C, 60 °C, and continuous condensation at 40 °C, respectively. The same figures for the VE profile were 6–12%, 4–6%, 7% and 14% (increase). These irregular trends in flexural modulus variation

associated with post-curing were also reported by Visco *et al.* [9] (VE profiles), being also in agreement with Cabral-Fonseca *et al.* [5].

3.6. In-plane shear response

Fig. 12 depicts the in-plane shear stress *vs.* strain behaviour of one representative specimen of both profiles for one of the ageing environments (W60), as an example of the changes exhibited by the in-plane shear strength (τ) and modulus (G).

The variations in both properties are evident with the ageing time, especially in what concerns the maximum shear stress (τ_{max}). In this case, the much better performance of the VE profile is clearer than in the previous tests, as the shear properties are more matrix-dependent, highlighting the differences in short- and long-term performance of both types of polymer matrices.

Fig. 13 summarizes the effects of hygrothermal ageing on the shear modulus and strength (average ± standard deviation) of the UP and VE profiles for all ageing environments. The overall effects of hygrothermal ageing on the in-plane shear strength corresponded to a general monotonic degradation trend, with a clear strength reduction with increasing time and temperature of exposure. These effects are usually attributed to plasticization of the polymer matrix (clearly identified in DMA tests, *cf.* section 3.3) and other degradation mechanisms, such as micro-cracking, that can contribute to the reduction of the shear properties [32]. As mentioned above, the VE resin afforded superior performance in all ageing environments.

For the 20 °C and 40 °C immersions, a gradual reduction of in-plane shear strength of both profiles is noted up to 9 months, which then progressed to a stabilization plateau, analogously to the flexural strength. For the 60 °C immersions, reductions of in-plane shear strength occurred in a more continuous way – a stabilization plateau was not visible throughout the whole ageing period. Similarly to what was observed for flexural strength, no apparent recovery was found for the in-plane shear strength of both profiles, which should (again) stem from the high influence of the degradation of the polymer matrices and of the fibre–matrix interfaces in these matrix-dominated properties. After 24 months of exposure, the in-plane shear strength of the UP profile presented reductions of 4–13%, 25–27%, 36–45%, and 15% for immersions at 20 °C, 40 °C, 60 °C, and continuous condensation at 40 °C, respectively; for the VE profile, those figures were 12–13%, 17–21%, 22–23%, and 15%. These values are consistent with results of similar tests conducted by Grammatikos *et al.* [32] on the in-plane shear properties of a pultruded unsaturated polyester GFRP flat sheet; despite the similarities in terms of temperature dependence of the shear strength reduction, the authors of that study also reported evidence of strength increase due to additional cross-linking associated with post-curing effects in the matrix after 112 days. While additional cross-linking of the matrix is likely to have also occurred in the present research, it did not result in an observable strength increase. These differences are attributed to the shorter exposure periods (maximum of 6 months) used in their tests, which did not allow to promote the effects resulting from longer exposure periods, as well as the lower glass fibre content in the studied laminate, which may have increased the magnitude of the post-curing effects.

Regarding the in-plane shear modulus, an apparent monotonic reduction is noted up to 9 months for most of the ageing environments, followed by a significant recovery up to 24 months. Temperature dependence is also noted, however to a lesser extent compared to shear strength. The variation pattern of shear modulus was more irregular and had higher scatter compared to shear strength. This was due to the method (video-extensometer) used to measure the shear strain, which captures the full shear stress *vs.* strain relationship, but presents lower precision for low levels of strain. The highest reductions were found at 9 months and at the higher temperature environments, ranging from 20 to 28% in the UP profile and 12–18% in the VE profile. For this particular property, the effects of hygrothermal ageing at the longer exposure periods were more pronounced in the VE profile, especially for the higher immersion temperature; this is attributed to the susceptibility of the UP resin to post-curing effects, as reported in the DMA tests.

At the end of the experiments, the in-plane shear modulus of the UP-profile presented a 5–10% increase in the 20 °C immersion environments. For immersion at 40 °C, the shear modulus increased 8% in W40, while it presented a minute reduction of 2% in S40. In W60, S60 and C40 environments, the shear modulus presented reductions of 10%, 4% and 2%, respectively. As for the VE profile, similar results were obtained, with increases of 2–4% in the 20 °C immersions. For the remaining environments, reductions of 2–7%, 15–18% and 4% were observed for immersions at 40 °C and 60 °C, and C40, respectively. The main trends of these results are quite similar to those obtained in the previously described work [32]. However, compared to that study, due to the desorption period, now the early monotonic reduction was attenuated and the property recovery was slightly higher, which is consistent with the other mechanical properties characterised so far.

3.7. Interlaminar shear response

Interlaminar shear strength (σ_{sbs}) provides insightful information about the degradation effects of the polymeric matrix at the interface

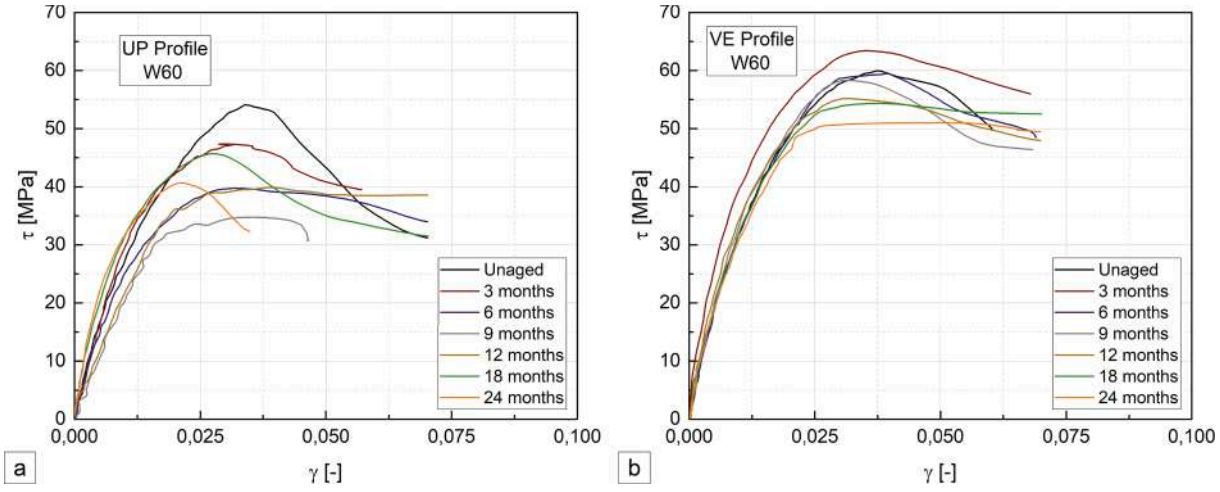

Fig. 12. In-plane shear stress *vs.* strain curves at different ageing times for immersion in water at 60 °C: (a) UP and (b) VE profiles (representative curves). (For interpretation of the references to colour in this figure legend, the reader is referred to the web version of this article.)

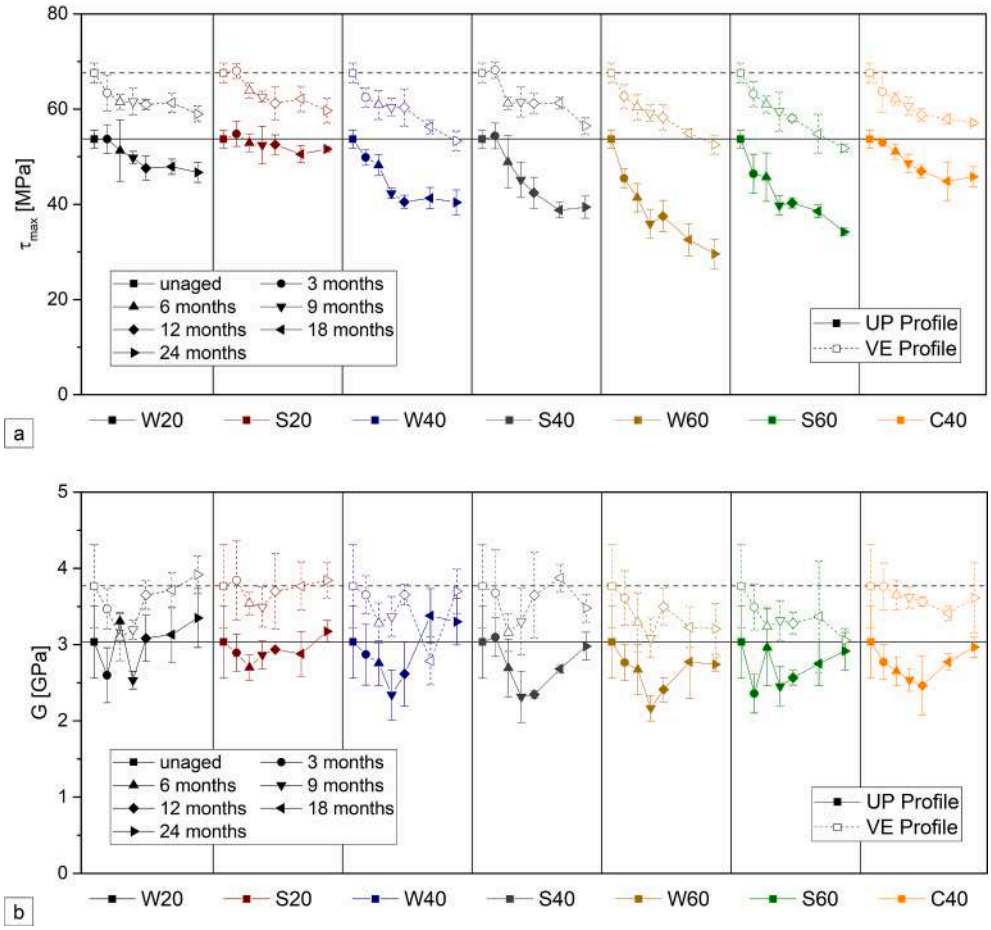

Fig. 13. Variations of (a) in-plane shear strength and (b) modulus for both profiles in the different ageing environments. (For interpretation of the references to colour in this figure legend, the reader is referred to the web version of this article.)

between reinforcing layers. Fig. 14 presents the interlaminar shear stress (σ_{sbs}) *vs*. midspan displacement (s) curves of representative specimens from both UP and VE profiles subjected to the W60 environment (as an example).

Even maintaining an approximately linear behaviour up to the peak stress, hygrothermal ageing caused a significant effect in the interlaminar shear strength of both profiles, which was more evident in the UP profile. Fig. 15 plots the variation of the interlaminar shear strength of the UP and VE profiles (average ± standard deviation) for all the ageing environments. The interlaminar shear strength of both profiles exhibited a general reduction trend with the ageing period, more or less continuous up to 9 months in all environments. Moreover, the strength reductions were more pronounced with increasing temperature, which is in agreement with other strength properties described earlier in this

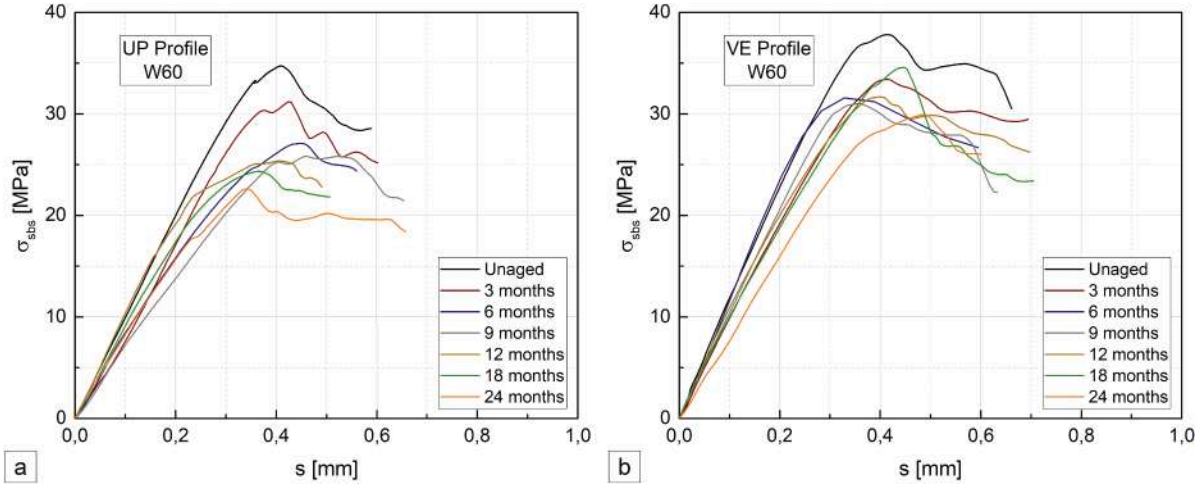

Fig. 14. Interlaminar shear stress *vs*. midspan displacement curves at different ageing times for immersion in water at 60 °C: (a) UP and (b) VE profiles (representative curves). (For interpretation of the references to colour in this figure legend, the reader is referred to the web version of this article.)

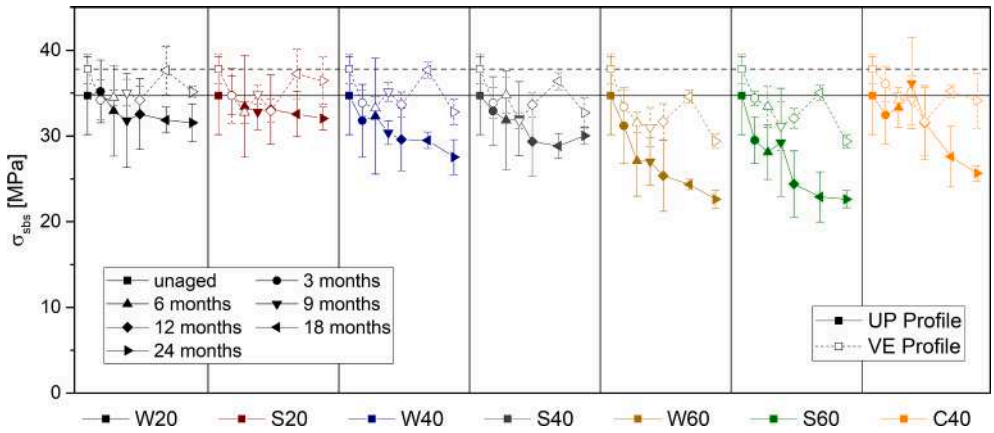

Fig. 15. Variation of interlaminar shear strength for both profiles in the different ageing environments. (For interpretation of the references to colour in this figure legend, the reader is referred to the web version of this article.)

paper, and also with results reported by Kharbari [35] and Cabral-Fonseca *et al.* [5]. However, in the latter study, after an initial and harsher reduction of interlaminar shear strength, a stabilisation plateau was attained. In the present study, the interlaminar shear strength of the UP profile gradually decreased, while that of the VE profile presented some recovery after 9 months, especially in the immersions at 20 °C; this non-monotonic variation is also consistent with the aforementioned occurrence of post-curing effects, also identified in the flexural properties. Kharbari [35] also identified this increase in a VE-GFRP profile and attributed the higher degradation suffered at higher exposure temperatures not only to plasticization and hydrolysis effects, but also to interface debonding and microcrack coalescence to form transverse cracks, resulting in greater propensity for wicking of moisture; Kharbari also referred that long exposure periods (above 12 months) may cause degradation at the fibre level, through pitting, cracking and fibre dissolution (however, we could not confirm the occurrence of such phenomena in this study) [35]. It is also worth highlighting the overall good agreement between the variation of flexural and interlaminar shear strengths (also reported in [5]), most likely due to the influence of the resin matrix on both properties.

After 24 months of hygrothermal ageing, the UP profile presented interlaminar shear strength reductions of 8–9%, 14–21%, 34–35%, and 21% for immersions at 20 °C, 40 °C, 60 °C, and continuous condensation at 40 °C, respectively; for the VE profile, those figures were significantly lower, namely 4–7%, 13–14%, 21–22%, and 9%.

It is interesting to note that the effects of salt water immersions followed closely those caused by demineralised water immersions at the same temperature. In this case, and differently from other mechanical properties (e.g., flexural strength), salt appeared to have no evident effect on hindering hygrothermal deterioration. Yet, continuous condensation produced comparable effects to water immersion at 40 °C, as for all the other mechanical properties. The superior durability performance of the VE profile compared to the UP profile in terms of resistance to interlaminar shear failure is attested by (i) the higher strength in unaged condition, and (ii) the consistently lower strength reduction when subjected to the various hygrothermal ageing environments.

4. Summary

The two GFRP profiles exhibited approximately Fickian sorption behaviour with increased diffusivity at higher temperatures. As expected, the presence of salt seemed to hinder water uptake and the VE profile presented lower water uptake than the UP profile.

The DMA results were indicative of the occurrence of plasticization effects due to hygrothermal ageing, as well as post-curing phenomena in the polymeric matrix of both types of profiles. The overall effects of hygrothermal ageing on the T_g of both profiles were found to be limited.

Regarding mechanical characterisation, salt water caused similar (slightly lower) detrimental effects when compared to demineralised water immersion for similar exposure period. In addition, continuous condensation led to similar changes when comparing to water immersion at the same temperature.

Hygrothermal ageing negatively affected the tensile properties of the profiles: the tensile strength reduction was higher at initial periods of exposure, consistent with the higher initial water uptake, while the modulus reduction was more gradual. After 24 months, the highest reductions in strength occurred for water immersion at 60 °C, namely 45% and 33% for the UP and VE profiles, respectively.

Flexural strength reductions were also higher in the UP profile than in the VE profile, which presented property recovery after 12 months. The variations in flexural modulus did not follow any specific trend and showed no evidence of temperature dependency. The highest reductions in flexural strength were 48% and 37% for the UP and VE profiles, respectively.

The in-plane shear strength of both profiles showed an overall reduction with time and temperature for all ageing conditions. After 24 months, the in-plane shear strength of the UP profile had a maximum reduction of 45%, while that figure was only 23% for the VE profile. The shear modulus showed more irregular variations, with initial reductions for both profiles at higher temperatures, followed by an increase, reflecting the occurrence of post-curing effects on the polymeric matrices. The effects of hygrothermal ageing in interlaminar shear strength followed the same general trends of the in-plane shear strength.

5. Conclusions

This paper presented a comprehensive experimental study about the effects of hygrothermal ageing on pultruded GFRP profiles with two alternative resin matrices – UP and VE – used in civil engineering applications. This included their gravimetric analysis, thermo-mechanical analysis (DMA), and mechanical response in tension, flexure, in-plane shear and interlaminar shear, in which the effects of immersion in demineralized water and salt water at 20 °C, 40 °C and 60°, as well as continuous condensation at 40 °C, were quantified and compared.

Overall, the VE profile presented better durability performance than the UP profile in all mechanical tests, experiencing lower reductions for all properties, with such differences frequently being in the order of magnitude of about 10%. For both profiles, strength properties were consistently more affected by hygrothermal ageing than stiffness properties.

The wealth of experimental data presented in this paper are particularly useful for the calibration of suitable degradation models (e.g., as performed in [12]), which may be used to predict the long-term mechanical property retention of pultruded GFRP materials. Such

information is essential to the definition of appropriate recommendations to account for material degradation in the design of civil engineering GFRP structures.

CRediT authorship contribution statement

J.M. Sousa: Methodology, Formal analysis, Investigation, Writing - original draft, Writing - review & editing, Visualization. **M. Garrido:** Formal analysis, Investigation, Writing - original draft, Writing - review & editing, Validation. **J.R. Correia:** Conceptualization, Methodology, Supervision, Project administration, Funding acquisition. **S. Cabral-Fonseca:** Conceptualization, Methodology, Supervision.

Declaration of Competing Interest

The authors declare that they have no known competing financial interests or personal relationships that could have appeared to influence the work reported in this paper.

Acknowledgements

The authors wish to thank FCT (project PTDC/ECI-EGC/4609/2020) and CERIS for the funding. This work was also supported by the Portuguese National Innovation Agency (ANI) – EasyFloor Project (no. 2015/3480).

References

[1] Karbhari VM, Chin JW, Hunston D, Benmokrane B, Jusja T, Morgan R, et al. Durability gap analysis for fiber-reinforced polymer composites in civil infrastructure. J Compos Constr 2003;7:238–47.
[2] Chu W, Wu L, Karbhari VM. Durability evaluation of moderate temperature cured E-glass/vinylester systems. Compos Struct 2004;66:367–76.
[3] Karbhari VM. Durability of composites for civil structural applications. Boca Raton, Florida: Woodhead Publishing; 2007.
[4] Svetlik SL. An investigation in the hygrothermal degradation of an E-glass/vinylester composite in humid and immersion environments. PhD Thesis. UC San Diego; 2008.
[5] Cabral-Fonseca S, Correia JR, Rodrigues MP, Branco FA. Artificial accelerated ageing of GFRP pultruded profiles made of polyester and vinylester resins: Characterisation of physical-chemical and mechanical damage. Strain 2012;48:162–73.
[6] Grammatikos SA, Evernden M, Mitchels J, Zafari B, Mottram JT, Papanicolaou GC. On the response to hygrothermal aging of pultruded FRPs used in the civil engineering sector. Mater Des 2016;96:283–95.
[7] Karbhari VM, Zhang S. E-glass/vinylester composites in aqueous environments – I: experimental results. Appl Compos Mater 2003;10:19–48.
[8] Carra G, Carvelli V. Long-term bending performance and service life prediction of pultruded glass fibre reinforced polymer composites. Compos Struct 2015;127:308–15.
[9] Visco AM, Campo N, Cianciafara P. Comparison of seawater absorption properties of thermoset resins based composites. Compos Part A Appl Sci Manuf 2011;42:123–30.
[10] Lopez-Anido R, Harik I, Dutta P, Shahrooz B. Field performance evaluation of multiple fibre-reinforced polymer bridge deck systems over existing girders - Phase I. Report, Chapter 4, Ohio Department of Transportation, US Department of Transportation, Federal Highway Administration, USA; 2001.
[11] Karbhari VM. Dynamic mechanical analysis of the effect of water on E-glass vinylester composites. J Reinf Plast Compos 2006;25:631–44.
[12] Sousa JM. Durability of pultruded GFRP profiles and adhesively bonded connections between GFRP adherends. PhD Thesis in Civil Engineering, Instituto Superior Técnico, University of Lisbon, 2018, URL: http://coregroup.tecnico.ulisboa.pt/~coregroup.daemon/uploads/Theses/PhD_Joao_Sousa.pdf.
[13] ISO 175. Methods of test for the determination of the effects of immersion in liquid chemicals. Int Organ Stand; 2010.
[14] ASTM D 1141. Standard practice for the preparation of substitute ocean water. Am Soc Test Mater; 2013.
[15] ISO 6270. Paints and varnishes. Determination of resistance to humidity. Part 2: Continuous condensation (in-cabinet exposure with heated water reservoir). Int Organ Stand; 2017.
[16] ASTM D 5229. Standard test method for moisture absorption properties and equilibrium conditioning of polymer matrix composite materials. Am Soc Test Mater; 2014.
[17] ISO 6721. Plastics - Determination of dynamic mechanical properties - Part 1: General principles. Part 5: Flexural vibration - non-resonance method. Int Organ Stand; 2019.
[18] ASTM E 1640. Standard test method for assignment of the glass transition temperature by dynamic mechanical analysis. Am Soc Test Mater; 2018.
[19] ISO 527. Plastics - Determination of tensile properties. Part 1: General principles. Part 5: Test conditions for unidirectional fibre reinfoced plastic composites.Int Organ Stand; 2019.
[20] ISO 14125. Fiber-reinforced plastic composites - Determination of flexural properties. Int Organ Stand; 1998.
[21] ASTM D 5379/D 5379M. Standard test method for shear properties of composite materials by the V-notched beam method. Am Soc Test Mater; 2019.
[22] ASTM D 2344. Standard test method for short-beam strength of polymer matrix composite materials and their laminates. Am Soc Test Mater; 2016.
[23] ASTM E 1252. Standard practice for general techniques for obtaining spectra for qualitative analysis. Am Soc Test Mater; 2013.
[24] ISO 1172. Textile-glass-reinforced plastics – Prepegs, moulding compounds and laminates – determination of the textile-glass and mineral-filler content – calcination methods. Int Organ Stand; 1996.
[25] ISO 1183. Plastics – Methods for determining the density of non-cellular plastics. Part 1: Immersion method, liquid pyknometer and titration method. Int Organ Stand; 2019.
[26] Bao LR, Yee AF, Lee CYC. Moisture absorption and hygrothermal aging in a bismaleimide resin. Polymer 2001;42:7327–33.
[27] Jiang X, Kolstein H, Bijlaard FSK. Moisture diffusion in glass-fiber-reinforced polymer composite bridge under hot/wet environment. Compos Part B Eng 2013;45:407–16.
[28] Chin JW, Nguyen T, Aouadi K. Effects of environmental exposure on fiber-reinforced plastic (FRP) materials used in construction. J Compos Technol Res 1997;19:205–13.
[29] Bazli M, Ashrafi H, Oskouei AV. Effect of harsh environments on mechanical properties of GFRP pultruded profiles. Compos Part B Eng 2016;99:203–15.
[30] Karbhari VM, Rivera J, Zhang J. Low-temperature hygrothermal degradation of ambient cured E-glass/vinylester composites. J Appl Polym Sci 2002;86:2255–60.
[31] Jones F. Durability of reinforced plastics in liquid environments. In: Pritchard G, editor. Reinf. Plast. Durab., Woodhead Publishing, Cambridge; 1999, p. 70–110.
[32] Grammatikos SA, Zafari B, Evernden MC, Mottram JT, Mitchels JM. Moisture uptake characteristics of a pultruded fibre reinforced polymer flat sheet subjected to hot/wet aging. Polym Degrad Stab 2015;121:407–19.
[33] Aniskevich K, Aniskevich A, Arnautov A, Jansons J. Mechanical properties of pultruded glass fiber-reinforced plastic after moistening. Compos Struct 2012;94:2914–9.
[34] SP Systems. Guide to Composites. GTC-1-1908; n.d.
[35] Karbhari VM. E-glass/vinylester composites in aqueous environments: effects on short-beam shear strength. J Compos Constr 2004;8:148–56.